A Robust Observer Design for Nonlinear MIMO Plants using Time-Delayed Signals

Jeong Wan Lee and Pyung Hun Chang

Abstract : In this paper, a robust observer design method for nonlinear multi input multi-output (MIMO) plants is presented. This method enables the extension of the time delay observer (TDO) for nonlinear SISO plants in the phase variable form to MIMO plants. The designed TDO reconstructs the states of the plant expressed in the generalized observability canonical form (GOBCF), yet requiring neither the transformation of a plant, nor the real time computation of system nonlinearity. Consequently, when the TDO is used for several control schemes based on the transformed coordinates, the observer turned out to be computationally efficient and easy to design for nonlinear MIMO plants. In a simulation of a two-link manipulator with flexible joints, the control performances using TDO appeared to be similar to those using *actual* states and superior to those using numerical differentiation. Finally, in an experiment with a robot, it was confirmed that the TDO reconstructs the states reliably and TDO can be effectively used in a real closed-loop system.

Keywords : nonlinear observer time-delay control, coordinates transform, robust observer

I. Introduction

The design of a state observer is important in the control of nonlinear plants. In the literature, several observer structures based on different methods have been described: global linearization methods by coordinate transformation of state variables and the output injection [1]-[4], pseudolinearization methods [5][6], extended linearization methods [7], and variable structure approaches [8]-[11].

However, since all of linearization methods require an accurate plant model in order to make a linearized error dynamics either globally or locally, the accuracy of state reconstruction heavily depends on the accuracy of the model. Hence, for plants under larger parameter variations or model uncertainties, the observation accuracy could suffer. Even though observers based on variable structure approaches are shown to be very robust against bounded modeling errors, these observers also need a plant model for a sliding mode behavior.

Obtaining an *accurate* plant model is often a time-consuming and complex procedure, and the model thus obtained is still vulnerable to some inaccuracies; for instance, in the identification of robot model, there are inaccuracies in the inertia matrix, the Coriolis forces, and the gravitational components. In addition, if some of the observers above are used for control purposes, the burden for the real-time computation of the plant model could be quite large depending on the order and complexity of the model. For instance, in the observers based on the linearization methods or the variable structure methods, one needs to compute the nonlinear plant dynamics on a real-time basis. Although nowadays hardware architectures based on advanced microprocessors can support real-time routines of the above observer algorithms at sufficiently fast sampling rate, the problems of the hardware cost and implementation complexity are still non-trivial. Thus, this computational burden could obviously inhibit attempts to implement the observers to real systems.

With these issues in mind, the time delay observer (TDO) has been proposed for nonlinear single-input single-output (SISO) plants that are in the phase variable form [12]. The essential idea behind this observer came from the time delay control (TDC) [13] [14], that is, using time-delayed information (the value of the control inputs and the derivatives of state variables at the previous time step) to estimate both the plant dynamics and the uncertainties. Using this time delay estimation, the TDO has three merits for nonlinear SISO plants in the phase variable form: first, the TDO does not require *a priori* knowledge of a plant model, and hence the structure of the TDO is very simple (simplicity); second, the scheme does not require substantial amount of real-time computation in implementation due to the simplicity (numerical efficiency); third, the TDO is very robust to modeling errors (robustness).

In engineering practice, several plants must be dealt with in a nonlinear multi-input multi output (MIMO) plant, which includes robot dynamics with flexible joints, magnetic bearing systems, brushless DC motor systems, and so on. For these plants, the analysis and synthesis of an observer need to be based on the MIMO system theory. Several observers for nonlinear MIMO plants have been developed [2][7][8][10][15]. Among linearization methods, Krener and Respondek

Manuscript received : Sep. 17, 1998., Accepted : May. 18, 1999.
Jeong Wan Lee : Division of Mechanical Engineering and Mechatronics, Kangwon National University.
Pyung Hun Chang : Department of Mechanical Engineering, Korea Advanced Institute of Science and Technology.

[2] designed a global linearization observer for MIMO plants where the full Jacobian matrix of coordinate transform is integrable. Birk and Zeitz [15] designed nonlinear observers for MIMO plants using a transformation into the nonlinear observer canonical form and an extended linearization. In variable structure approaches, Walcott and Zak [10] proposed a variable structure observer for the MIMO plants that satisfy the matching condition, and Slotine *et al.* [8] extended a sliding observer for SISO plants in phase variable form to MIMO plants which meet the observability condition. However, similar to SISO case, most of the MIMO observers above require *a priori* knowledge of plant model for an observer design and real-time computation of nonlinearities in practical implementation.

In this paper, we extend the TDO method to general nonlinear MIMO plants. For this purpose, the transformation into generalized observability canonical form (GOBCF), introduced by [4], is used. More specifically, the TDO is designed on the basis of GOBCF, in the sense that it reconstructs the states of plants expressed in GOBCF. Nevertheless, coordinate transform is not required, if we use the model independence property of the TDO -- which is the essential idea underlying the effectiveness of the MIMO TDO described in this paper. This point will be explained more in detail in 2.4. Through this extension, what we want to contribute is twofold: to develop the TDO method so that it can be used for a wider class of nonlinear plants; and to confirm that the designed observer preserves the three merits of the TDO for SISO plants (simplicity, numerical efficiency, and robustness).

Since the intended purpose of the TDO is to control nonlinear plants, our main concern is to improve control performances when the TDO is connected with nonlinear controllers. In some plants, one possible way to implement nonlinear controllers in which only the plant output is available is to use the numerical differentiations of plant output, and then to estimate the states through the coordinate relations between the output derivatives and the actual states. How will the controller-TDO system perform compared with the controller-numerical differentiation system and the controller-actual states system? This is our immediate concern. Thus, the performances are compared by simulation using a two-link manipulator with flexible joints and experiment on a two-dof SCARA robot.

In the following section, the TDO will be proposed for nonlinear MIMO plants; and its convergence, numerical efficiency, and robustness will be analyzed. In Section 3, a simulation study will be undertaken to assure the validity of the observer. Section 4 will present the experimental results, followed by the conclusion in Section 5.

II. Time delay observer for MIMO plants

The TDO for nonlinear MIMO plants is based on the GOBCF proposed by Zeitz (1984). The resulting TDO does not require a plant to be transformed into the GOBCF; rather, the TDO reconstructs the states for the plant *as if* it were in the GOBCF. We will discuss this point in more detail in section 2.4.

1. Plant dynamics in the GOBCF

Although the design of the TDO does not require plants to be in the GOBCF, the GOBCF is derived to provide the background for the TDO. The nonlinear MIMO plant under consideration is of the following form:

$$\begin{aligned} \dot{\mathbf{x}} &= \mathbf{f}(\mathbf{x},\mathbf{u}), \\ \mathbf{y} &= \mathbf{h}(\mathbf{x},\mathbf{u}), \end{aligned} \tag{1}$$

where, $\mathbf{x} = \Re^n$, $\mathbf{u} = \Re^p$, and $\mathbf{y} = \Re^q$denote the state vector, the control input vector, and the output vector, respectively; $\mathbf{f}(\mathbf{x},\mathbf{u}) \in {}^{n\times 1}$ and $\mathbf{h}(\mathbf{x},\mathbf{u}) = [h_1(\mathbf{x},\mathbf{u}),h_2(\mathbf{x},\mathbf{u}),\cdots,h_q(\mathbf{x},\mathbf{u})]^T \in \Re^{q\times 1}$ are nonlinear functions, which are assumed to be sufficiently continuous and differentiable with respect to $\mathbf{x}$ and $\mathbf{u}$ (q subsystems with respect to the output $\mathbf{y}$).

For the plant to be expressed in the GOBCF, (1) must meet the observability condition in [4]:

$$\underbrace{\begin{bmatrix} \left(\frac{\partial h_1}{\partial \mathbf{x}}\right) \\ \left(\frac{\partial N h_1}{\partial \mathbf{x}}\right) \\ \vdots \\ \left(\frac{\partial N^{n_1-1} h_1}{\partial \mathbf{x}}\right) \end{bmatrix}}_{\mathbf{Q}_1(\mathbf{x},\bar{\mathbf{u}})} = n_1 \text{ ; for } i = 1,\cdots,q, \sum_{k=1}^{q} n_k = n, \tag{2}$$

where $\mathbf{Q}(\mathbf{x},\bar{\mathbf{u}}) = [\mathbf{Q}_1^T(\mathbf{x},\bar{\mathbf{u}}),\cdots,\mathbf{Q}_q^T(\mathbf{x},\bar{\mathbf{u}})]^T$ denotes the observability matrix, N the differential operator defined as

$$\begin{aligned} N^k h_i &:= \left[\frac{\partial}{\partial \mathbf{x}} N^{k-1} h_i\right]^T \mathbf{f} + \left[\frac{\partial}{\partial \mathbf{x}} N^{k-1} h_i\right]^T \bar{\mathbf{u}}, \\ N^0 h_i &= h_i, \text{ and } \bar{\mathbf{u}} = [\mathbf{u}, \dot{\mathbf{u}}, \cdots, \mathbf{u}^{(n-1)}]^T, \end{aligned} \tag{3}$$

and n_i denotes the *selected degree* of i-th output. Notice that given a nonlinear MIMO plants (1), the GOBCF in general is not necessarily unique, the dimension of i-th subsystem n_i --- and hence $\mathbf{Q}(\mathbf{x}, \bar{\mathbf{u}})$ — could differ, thereby forming different $\mathbf{Q}(\mathbf{x}, \bar{\mathbf{u}})$ [4].

The coordinate transformation [4]

$$\underbrace{\begin{bmatrix} \mathbf{z}_1 \\ \vdots \\ \mathbf{z}_q \end{bmatrix}}_{z(t)} = \underbrace{\begin{bmatrix} \mathbf{v}_1(\mathbf{x},\bar{\mathbf{u}}) \\ \vdots \\ \mathbf{v}_q(\mathbf{x},\bar{\mathbf{u}}) \end{bmatrix}}_{v(\mathbf{x},\bar{\mathbf{u}})}, \text{with } \mathbf{v}_i(\mathbf{x},\bar{\mathbf{u}}) = \begin{bmatrix} N^0 h_i(\mathbf{x},\bar{\mathbf{u}}) \\ \vdots \\ N^{n_i-1} h_i(\mathbf{x},\bar{\mathbf{u}}) \end{bmatrix}, \tag{4}$$

then renders (1) to the following GOBCF:

$$\underbrace{\begin{bmatrix}\dot{\mathbf{z}}_1\\ \vdots\\ \dot{\mathbf{z}}_q\end{bmatrix}}_{\dot{\mathbf{z}}} = \underbrace{\begin{bmatrix}\mathbf{E}_{n_1} & & \mathbf{0}\\ & \ddots & \\ \mathbf{0} & & \mathbf{E}_{n_q}\end{bmatrix}}_{\mathbf{E}}\underbrace{\begin{bmatrix}\mathbf{z}_1\\ \vdots\\ \mathbf{z}_q\end{bmatrix}}_{\mathbf{z}} + \underbrace{\begin{bmatrix}\mathbf{a}_1(\mathbf{z},\bar{\mathbf{u}})\\ \vdots\\ \mathbf{a}_q(\mathbf{z},\bar{\mathbf{u}})\end{bmatrix}}_{\mathbf{a}(\mathbf{z},\bar{\mathbf{u}})},$$

$$\mathbf{y} = \underbrace{\begin{bmatrix}\mathbf{C}_1 & & \mathbf{0}\\ & \ddots & \\ \mathbf{0} & & \mathbf{C}_q\end{bmatrix}}_{\mathbf{C}}\underbrace{\begin{bmatrix}\mathbf{z}_1\\ \vdots\\ \mathbf{z}_q\end{bmatrix}}_{\mathbf{z}}, \tag{5}$$

with

$$\mathbf{z}_i = \begin{bmatrix}z_{i1}\\ \vdots\\ z_{in_i}\end{bmatrix}, \mathbf{E}_{n_i} = \begin{bmatrix}\mathbf{0}_{(n_i-1)\times 1} & \vdots & \mathbf{I}_{(n_i-1)}\\ 0 & \cdots & 0\end{bmatrix}, \mathbf{C}_i = \begin{bmatrix}1 & \vdots & \mathbf{0}_{1\times(n_i-1)}\end{bmatrix}, \mathbf{a}_i(\mathbf{z},\bar{\mathbf{u}}) = \begin{bmatrix}0\\ \vdots\\ a_i(\mathbf{z},\bar{\mathbf{u}})\end{bmatrix}.$$

Note that it is assumed that the coordinate transformation $\mathbf{v}(\mathbf{x})$ in (4) is a smooth function, and its inverse $\mathbf{v}^{-1}(\mathbf{x})$ exists and is smooth (in other words, $\mathbf{v}(\mathbf{x})$ is a diffeomorphism). Then, the term $a_i(\mathbf{z}, \bar{\mathbf{u}})$ can be determined by

$$a_i(\mathbf{z},\bar{\mathbf{u}}) = N^{n_i}h_i(\mathbf{x},\bar{\mathbf{u}})\Big|_{\mathbf{x}=\mathbf{v}^{-1}(\mathbf{z},\bar{\mathbf{u}})}. \tag{6}$$

Note that determining $a_i(\mathbf{z}, \bar{\mathbf{u}})$ requires the inverse transformation:

$$\mathbf{x} = \mathbf{v}^{-1}(\mathbf{z},\bar{\mathbf{u}}), \tag{7}$$

which in turn requires a plant model.

2. Derivation of TDO

In the transformed coordinate, suppose that for each subsystem of (5) an observer of the following form is available:

$$\dot{\hat{\mathbf{z}}}_i = \mathbf{E}_{n_i}\hat{\mathbf{z}}_i + \mathbf{a}_i(\mathbf{z},\bar{\mathbf{u}}) + \mathbf{K}_i(\mathbf{C}_i\hat{\mathbf{z}}_i - \mathbf{y}_i), \tag{8}$$

where $\hat{\mathbf{z}}_i \in \Re^{n_i}$ denotes the reconstructed state vector for each subsystem $\mathbf{z}_i$, and $\mathbf{K}_i \in \Re^{n_i\times 1}$ the observer gain matrix for each subsystem. Then the subsystem observation error $\mathbf{e}_i = \hat{\mathbf{z}}_i - \mathbf{z}_i$ has an exponentially convergent dynamics as follows:

$$\dot{\mathbf{e}}_i = (\mathbf{E}_{n_i} + \mathbf{K}_i\mathbf{C}_i)\mathbf{e}_i, \tag{9}$$

where an arbitrary convergence speed can be achieved by a suitable choice of $\mathbf{K}_i$.

In order to realize the observer, one must be able to estimate the uncertainty, $a_i(\mathbf{z},\bar{\mathbf{u}})$ in $\mathbf{a}_i(\mathbf{z},\bar{\mathbf{u}})$. To this end, we have adopted from TDC [13] an especially efficient estimation method: first, use the fact that $a_i(\mathbf{z},\bar{\mathbf{u}})$ may be assumed mostly as a continuous function, from which we can derive the following formula, for a sufficiently small time delay L,

$$a_i(\mathbf{z},\bar{\mathbf{u}}) \approx a_i(\mathbf{z}_{(t-L)},\bar{\mathbf{u}}_{(t-L)}) \tag{10}$$

Secondly, using (5) and (10), obtain the following estimation for the uncertainties, $a_i(\mathbf{z},\bar{\mathbf{u}})$:

$$a_i(\mathbf{z},\bar{\mathbf{u}}) = \dot{z}_{in_i} \approx \dot{z}_{in_i(t-L)}. \tag{11}$$

In the digital implementation, for which TDO is intended, the value of L is normally set to be the sampling time T_s. If the convergence speed of i-th subsystem error dynamics (9) is made much faster than that of the dynamics of $a_i(\mathbf{z},\bar{\mathbf{u}})$, the following holds:

$$a_i(\mathbf{z},\bar{\mathbf{u}}) = \ddot{\hat{z}}_{in_i(t-L)}. \tag{12}$$

Finally, substituting (12) into (8) and introducing a constant α_i leads to the following TDO equation for i-th subsystem,

$$\dot{\hat{\mathbf{z}}}_i = \mathbf{E}_{n_i}\hat{\mathbf{z}}_i + \alpha_i\begin{bmatrix}\mathbf{0}_{1\times(n_i-1)} & \vdots & \ddot{\hat{z}}_{in_i(t-L)}\end{bmatrix}^T + \mathbf{K}_i(\mathbf{C}_i\hat{\mathbf{z}}_i - \mathbf{y}_i). \tag{13}$$

The TDO equation for the total system is then

$$\dot{\hat{\mathbf{z}}} = \mathbf{E}\hat{\mathbf{z}} + \begin{bmatrix}\alpha_1\begin{bmatrix}\mathbf{0}_{1\times(n_1-1)} & \vdots & \ddot{\hat{z}}_{1n_1(t-L)}\end{bmatrix}^T\\ \vdots\\ \alpha_q\begin{bmatrix}\mathbf{0}_{1\times(n_q-1)} & \vdots & \ddot{\hat{z}}_{qn_q(t-L)}\end{bmatrix}^T\end{bmatrix} + \begin{bmatrix}\mathbf{K}_1(\mathbf{C}_1\hat{\mathbf{z}}_1 - \mathbf{y}_1)\\ \vdots\\ \mathbf{K}_q(\mathbf{C}_q\hat{\mathbf{z}}_q - \mathbf{y}_q)\end{bmatrix}. \tag{14}$$

The idea behind introducing the constant α_i is based on the attempt by [16], that is, introducing α_i has the effect of using a low pass filter. This point was explained in more detail in [12].

3. Convergence of estimates

The observation error dynamics is derived in Lemma 1, and the conditions for its convergence are provided in Theorem 1; proofs are presented in the appendix.

Lemma 1: The TDO in (14), if used for the nonlinear plants in (5), has the following observation error dynamics for each subsystem:

$$\dot{\tilde{\mathbf{e}}}_i = \tilde{\mathbf{A}}_i\tilde{\mathbf{e}}_i + \tilde{\mathbf{B}}_i\gamma_i(\mathbf{z},\bar{\mathbf{u}},L), \tag{15}$$

where

$$\tilde{\mathbf{e}}_i = \begin{bmatrix}e_{i1}\\ \vdots\\ e_{in_i}\end{bmatrix} \text{ with } \tilde{e}_{in_i+1} = \dot{\tilde{e}}_{in_i}, \tilde{\mathbf{A}}_i = \begin{bmatrix}K_{i1} & 1 & 0 & \cdots & 0\\ K_{i2} & 0 & 1 & \cdots & 0\\ \vdots & \vdots & & \ddots & \vdots\\ K_{in_i-1} & 0 & 0 & \cdots & 1\\ K_{in_i} & 0 & 0 & \cdots & 0\end{bmatrix}, \tilde{\mathbf{B}}_i = \begin{bmatrix}0_{n_i\times 1}\\ \vdots\\ 1\end{bmatrix}, \tag{16}$$

$$\gamma_i(\mathbf{z},\bar{\mathbf{u}},L) = \left(\frac{(1-\alpha_i)}{\alpha_i L}a_i(\mathbf{z},\bar{\mathbf{u}}) + \psi_i(L) - \frac{\alpha_i}{\alpha_i L}\phi_i(\mathbf{z},\bar{\mathbf{u}},L)\right) \tag{17}$$

with $\psi_i(L) = \frac{\ddot{\tilde{e}}_{in_i} - \ddot{\tilde{e}}_{in_i(t-L)}}{L} - \dddot{\tilde{e}}_{in_i}$ and $\phi_i(\mathbf{z},\bar{\mathbf{u}},L) = a_i(\mathbf{z},\bar{\mathbf{u}}) - a_i(\mathbf{z}_{(t-L)},\bar{\mathbf{u}}_{(t-L)})$.

Theorem 1: In the subsystem error dynamics (15), if

1) for all $t > 0$, $|a_i(\mathbf{z},\bar{\mathbf{u}})| < P_i < \infty$, $|\psi_i(L)| < \Psi_i < \infty$, and $|\phi_i(\mathbf{z},\bar{\mathbf{u}})| < \Phi_i < \infty$,

2) every eigenvalue of $\tilde{\mathbf{A}}_i$ is distinct and has a negative real part, be it real or complex,

then the estimation error for each subsystem is

exponentially convergent to the open domain

$$B_i(\delta_i) = \{\tilde{\mathbf{e}}_i : 0 \le \|\tilde{\mathbf{e}}_i\| < \delta_i\}, \tag{18}$$

where

$$\delta_i = \|\mathbf{T}_i^{-1}\|\|\mathbf{T}_i\| \sqrt{\frac{(1 + K_{i1}^2 + \cdots + K_{in_i-1}^2)}{K_{in_i}^2}} \beta_i,$$

$$\text{with } \beta_i = (1-\alpha_i)P_i + \alpha_i L \Psi_i + \alpha_i \Phi_i,$$

and T_i denotes a transform matrix to diagonalize $\tilde{\mathbf{A}}_i$. In addition, the steady state estimation error, $\|\tilde{\mathbf{e}}_{i_{ss}}\|$ is bounded as follows:

$$\|\tilde{\mathbf{e}}_{i_{ss}}\| < \sqrt{\frac{(1 + K_{i1}^2 + \cdots + K_{in_i-1}^2)}{K_{in_i}^2}} \beta_i. \tag{19}$$

Remark 1 : The relationship (18) in Theorem 1 may be used to estimate $\|\tilde{\mathbf{e}}_i\|$: given $\mathbf{K}_i$, and α_i, and L, they can be used to estimate $\|\mathbf{T}_i^{-1}\|\|\mathbf{T}_i\|$, Ψ_i, and Φ_i, and ultimately $\|\tilde{\mathbf{e}}_{i_{ss}}\|$.

Remark 2 : If the coordinate transformation $\mathbf{z} = \mathbf{v}(\mathbf{x}, \bar{\mathbf{u}})$ is one-to-one mapping, then the convergence of the estimation error in GOBCF, $\tilde{\mathbf{e}} = \hat{\mathbf{z}} - \mathbf{z}$, guarantees the convergence of the observation error in the initial coordinate, $\hat{\mathbf{x}} - \mathbf{x}$.

4. Numerical efficiency

In this subsection, we emphasize design simplicity and implementation practicality (i.e., using a microprocessor). As seen in (14), the design of the TDO does *not* require the knowledge of nonlinearity $a_i(\mathbf{z}, \bar{\mathbf{u}})$, instead it only requires the simple algorithm of time delay estimation. In some plants, the form of $a_i(\mathbf{z}, \bar{\mathbf{u}})$ is very complex and the computational amount of it can be large. The computation effort at each sampling amounts to $(n+2q)$ multiplications and $(n+2q)$ additions. For example, let us see the equation (24) of two-dof manipulator with flexible joints. In this case, the total computational amount of the TDO is 12 multiplications and 12 additions; which is about one eighth of that of nonlinear observer using global linearization methods.

The states that the TDO reconstructs are those for the plant in the GOBCF; yet, the TDO does *not* require the transformation of the plant in (1) because the only information the TDO requires is $\mathbf{y}$, which is already available from (1). Since the intended purpose of using the TDO is primarily to control nonlinear plants, one may do so in the transformed coordinate if the coordinate transformation is diffeomorphism [17]. For instance, in several control techniques based on *feedback linearization* [17] and on the *sliding mode control* [18], control actions can be made by using the states of the transformed coordinate. As seen in (14), the TDO can be designed even if the transformation is not known since it only needs the transformability condition. Therefore, if the TDO is used for the above control structures, certain design and implementation advantages are produced.

If in some situations, however, the states are reconstructed in the initial coordinate, $\hat{\mathbf{x}}(t)$ can be obtained by using the inverse transformation (7):

$$\hat{\mathbf{x}} = \mathbf{v}^{-1}(\hat{\mathbf{z}}, \bar{\mathbf{u}}) \tag{20}$$

Note that the inverse transformation requires both the knowledge of the plant model and the computation based on it and that it may also deteriorate reconstruction accuracy as modeling errors become larger.

5. Robustness issues

In order to test the robustness of TDO against plant uncertainty, we use the result of [12] and equation (19). As seen in (19), the steady state observation error due to plant uncertainty is mainly dependent on the observer gain $\mathbf{K}$ and α, which also affect the sensitivity to sensor noise [12]. Accordingly, $\sqrt{(1 + K_{i1}^2 + \cdots K_{in_i-1}^2)/K_{in_i}}$ decreasing and increasing α_i close to 1 improves the performance robustness to plant uncertainty but makes the observer more sensitive to measurement noise whereas increasing $\sqrt{(1 + K_{i1}^2 + \cdots K_{in_i-1}^2)/K_{in_i}}$ and decreasing α_i reverses the balance. Therefore careful tuning α_i of is required for a good compromise between robustness to uncertainty and sensitivity to measurement noise.

Moreover, from our practical experiences in some simulations and experiments, we have found that faster sampling rate improves both the performance robustness to plant uncertainty and the sensitivity to measurement noise. Fortunately, owing to its substantial simplicity and numerical efficiency, to increase the sampling rate is relatively easy with the TDO.

6. Gain selection method

The parameters, α_i, L, and $\mathbf{K}_i$, can be selected so that the eigenvalues of error dynamics in (15) may be placed at prescribed locations. The procedure may be summarized as follows:

1) Obtain the characteristic equation from (15),

$$s^{n_i+1} + \left[\frac{1-\alpha_i}{\alpha_i L} + K_{i1}\right]s^{n_i} + \left[\frac{1-\alpha_i}{\alpha_i L}K_{i1} + K_{i2}\right]s^{n_i-1} + \cdots + \left[\frac{1-\alpha_i}{\alpha_i L}K_{in_i-2} + K_{in_i-1}\right]s^2 + \left[\frac{1-\alpha_i}{\alpha_i L}K_{in_i-1}\right]s + \frac{K_{\omega_i}}{\alpha_i L} = 0, \tag{21}$$

and a characteristic equation with desired eigenvalues,

$$s^{n_i+1} + A_1 s^{n_i} + A_2 s^{n_i-1} + \cdots + A_{n_i} s + A_{n_i+1} = 0, \tag{22}$$

2) Compare, term by term, the coefficients of (21) and (22) and eliminate $\frac{1-\alpha_i}{\alpha_i L}, K_{i2}, \cdots, K_{in_i-1}$, successively, to obtain an n_i-th order polynomial equation of p_i:

$$A_{n_i} + A_{n_i-1} p_i + A_{n_i-2} p_i^2 + \cdots + A_1 p_i^{n_i-1} + p_i^{n_i} = 0, \quad (23)$$

where $p_i \equiv K_{i1} - A_1$.

3) Solve (23) for p_i (equivalently, K_{i1}).

4) Select a sufficiently small L considering CPU power.

5) Solve the remaining parameters by comparing the coefficients of (21) with those of (22), which are obtained as follows:

$$\begin{aligned}
\alpha_i &= \frac{1}{(A_i - K_{i1})L + 1} \\
K_{i2} &= A_2 - \frac{1-\alpha_i}{\alpha_i L} K_{i2} \\
K_{i2} &= A_2 - \frac{1-\alpha_i}{\alpha_i L} K_{i2} \\
&\cdots\cdots \\
K_{in_i-1} &= A_{n-1} - \frac{1-\alpha_i}{\alpha_i L} K_{in_i-2} \\
K_{in_i} &= \alpha_i L A_{n+1}
\end{aligned} \quad (24)$$

6) After experimenting for the sensitivity to noise, adjust the eigenvalues and repeat the procedure until a prescribed specification is satisfied.

7) Follow the procedure above, for i=1 to q

III. Simulation

The TDO is implemented for the position control of two-dof manipulator with flexible joints. Through this simulation, we want to verify the effectiveness and applicability of the TDO, and to test the robustness of the TDO against modeling error.

1. Description of plant

The example we will present is a two-dof manipulator with flexible joints (see [19]) whose schematic diagram is given in Fig. 1 and modeled as follows:

$$\begin{aligned}
\ddot{x}_1 &= -\frac{k_1(x_1 - x_3) - h_2 \sin(2x_2)\dot{x}_1\dot{x}_2}{h_5 + h_2 \cos^2(x_2)}, \\
\ddot{x}_2 &= -h_1\left(k_2(x_2 - x_4) + h_6 \cos(x_2) + \frac{h_2}{2}\sin(2x_2)\dot{x}_1^2\right), \\
\ddot{x}_3 &= \frac{u_1 + k_1(x_1 - x_3)}{h_3}, \\
\ddot{x}_4 &= \frac{u_2 + k_2(x_2 - x_4)}{h_4},
\end{aligned} \quad (25)$$

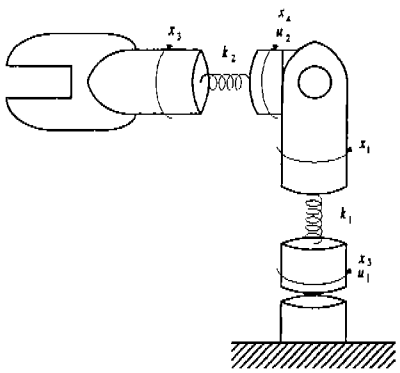

Fig. 1. Schematic diagram of two-dof manipulator with flexible joints.

where x_1 and x_2 denote the positions of the first and second flexible links; x_3 and x_4 the positions of the first and second motor shafts; u_1 and u_2 the first and second control inputs, respectively; h_i the parameter consisting of the mass, the moment of inertia, the gravity; k_i and the spring constant of the flexible links. The numerical values of parameters in equation (25) used for simulation are listed as follows:

$$\begin{aligned}
h_1 &= 0.095(kgm^2)^{-1} & h_2 &= 22.058 kgm^2 \\
h_3 &= 23.296 kgm^2 & h_4 &= 70.656 kgm^2 \\
h_5 &= 0.084 kgm^2 & h_6 &= 291.106 kgm^2 \\
k_1 &= 29800 kgm^2/s^2 & k_2 &= 14210 kgm^2/s^2
\end{aligned}$$

In this example, assuming that all the positions of flexible links are available, (25) can be expressed in the nonlinear MIMO state equation form as (1) with the state vector $\mathbf{x} = [x_1, \dot{x}_1, x_2, \dot{x}_2, x_3, \dot{x}_3, x_4, \dot{x}_4]^T$ and output vector $\mathbf{y} = [x_1, x_2]^T$.

The observability matrix (2) can be obtained by computation, which is rank 8 for the parameters listed above. Therefore, the system (25) is transformable into the GOBCF. Coordinate transformation,

$$\begin{aligned}
&z_{11} = x_1, z_{12} = \dot{x}_1, z_{21} = x_2, z_{22} = \dot{x}_2, \\
&z_{13} = -\frac{k_1(x_1 - x_3) - h_2 \sin(2x_2)\dot{x}_1\dot{x}_2}{(h_5 + h_2 \cos^2(x_2))}, \\
&z_{14} = \frac{2h_2 \sin(2x_2)[h_2 \sin(2x_2)\dot{x}_1\dot{x}_2 - k_1(x_1 - x_3)]\dot{x}_2}{(h_5 + h_2 \cos^2(x_2))^2} \\
&\quad + \frac{2h_2 \cos(2x_2)\dot{x}_1\dot{x}_2^2 - k_1(\dot{x}_1 - \dot{x}_3)}{(h_5 + h_2 \cos^2(x_2))} \\
&\quad + \frac{h_1 h_2 \sin(2x_2)[k_2(x_2 - x_4) + h_6 \cos(x_2) + \frac{h_2}{2}\sin(2x_2)\dot{x}_1^2]\dot{x}_1}{(h_5 + h_2 \cos^2(x_2))}, \\
&z_{23} = -h_1\left[k_2(x_2 - x_4) + h_6 \cos(x_2) + \frac{h_2}{2}\sin(2x_2)\dot{x}_1^2\right] \\
&z_{24} = -h_1\left[\left(k_2 - h_6 \sin(x_2) + h_2 \cos(2x_2)\dot{x}_1^2\right)\dot{x}_2 - k_2\dot{x}_4\right] \\
&\quad + \frac{h_1 h_2 \sin(2x_2)[k_1(x_1 - x_3) - h_2 \sin(2x_2)\dot{x}_1\dot{x}_2]\dot{x}_1}{(h_5 + h_2 \cos^2(x_2))},
\end{aligned} \quad (26)$$

renders (25) to the GOBCF:

$$\begin{aligned}
\begin{bmatrix} \dot{\mathbf{z}}_1 \\ \dot{\mathbf{z}}_2 \end{bmatrix} &= \begin{bmatrix} \mathbf{E}_4 & \mathbf{0} \\ \mathbf{0} & \mathbf{E}_4 \end{bmatrix} \begin{bmatrix} \mathbf{z}_1 \\ \mathbf{z}_2 \end{bmatrix} - \begin{bmatrix} \mathbf{a}_1(\mathbf{z}, \bar{\mathbf{u}}) \\ \mathbf{a}_2(\mathbf{z}, \bar{\mathbf{u}}) \end{bmatrix}, \\
\mathbf{y} &= [z_{11}, z_{21}]^T,
\end{aligned} \quad (27)$$

where

$$\begin{aligned}
a_1(\mathbf{z}, \bar{\mathbf{u}}) = &-k_1 z_{13} + 6h_2 \cos(2z_{21})(z_{13} z_{22}^2 + z_{12} z_{22} z_{23}) \\
&+ h_2 \sin(2z_{21})(3z_{14} z_{22} + 3z_{13} z_{23} + 3z_{12} z_{24} - 4z_{12} z_{22}^3) \\
&- \frac{k_1}{h_3}(h_5 + h_2 \cos^2(2z_{21}))z_{13} + \\
&\frac{k_1 h_2}{h_3}\sin(2z_{21}) z_{12} z_{22} + \frac{k_1}{h_3} u_1 \\
&\hline \\
&(h_5 + h_2 \cos^2(2z_{21})),
\end{aligned}$$

$$\begin{aligned}
a_2(\mathbf{z}, \bar{\mathbf{u}}) = &\, h_1\left[h_6\left(\cos(z_{21}) z_{22}^2 + \sin(z_{21}) z_{23}\right) - k_2 z_{23}\right] \\
&+ h_1 h_2 \sin(2z_{21})\left(2z_{12}^2 z_{22}^2 - z_{13}^2 - z_{12} z_{24}\right) \\
&- h_1 h_2 \cos(2z_{21})\left(4z_{12} z_{13} z_{22} + z_{12}^2 z_{23}\right)
\end{aligned} \quad (28)$$

$$-\left(\frac{k_2}{h_4}z_{23}+\frac{h_1k_2h_6}{h_4}\cos(z_{21})+\frac{h_1h_2k_2}{2h_4}\sin(2z_{21})z_{12}^{\,2}-\frac{h_1k_2}{h_4}u_2\right)$$

The corresponding TDO for the GOBCF (27) can be designed by equation (13), which completes the design procedure. If reconstruction of the initial states is required, it can be obtained using inverse coordinate transform.

2. Simulation conditions

With the initial condition, $\mathbf{x}=[0,0\frac{\pi}{2},0,0,0,0,0]^T$, we applied a step-type command for the simulation and then adopted two control algorithms: an I/O linearization controller (IOLC) algorithm [17] and an I/O linearization using a time delay control (IOLTDC) algorithm [16]. The IOLC requires the computation of the system nonlinearity in the initial coordinate, **x**, or in the transformed coordinate, **z**, in order to obtain a linear input/output behavior. In contrast, the IOLTDC requires little *a priori* knowledge of the dynamics of the system. The uncertainties in the dynamics are compensated for through the time delay estimation using the measurement or estimation of $\mathbf{z}$ and $\dot{\mathbf{z}}$. Therefore, the IOLTDC utilizes the states of the transformed coordinate, **z**, not those of the initial coordinate, **x**.

In order to compare the performances, we applied these controllers together while utilizing the actual states (**x** and **z**), the observed states by the TDO, and the estimated states by numerical differentiations of plant output. We will use the responses of the system to the control utilizing the actual states as a benchmark for the control utilizing the TDO and numerical differentiations. Then we will do a comparative study of the performances of the three control systems. The TDO gains will be as follows: $K_{11}=-380$, $K_{21}=-57610$, $K_{22}=-14423$, $K_{13}=-5456737$, $K_{23}=682100$, $K_{14}=-4862789$, $K_{24}=-486278$ $\alpha_1=\alpha_2=0.8$, and $L=0.001s$. From this simulation work we will know if the TDO works properly when connected to the controllers.

3. Simulation results

In the first simulation, we applied the IOLC in two different cases: without a modeling error and with a 30% modeling error. A 30% modeling error was generated by setting the h_i's of the model to be 0.7 times smaller than those of the plant. Figs. 2 and 3 show the plot representing the step responses of the systems in these two cases. These figures indicate the performances of the controller-TDO system and the controller-numerical differentiation system versus those of the benchmark.

As shown in Fig. 2, in the system without the modeling error, even though the response of the controller-TDO system in link 1 is slightly slower than that of the benchmark, the performance of the controller-TDO system is adequate from a practical

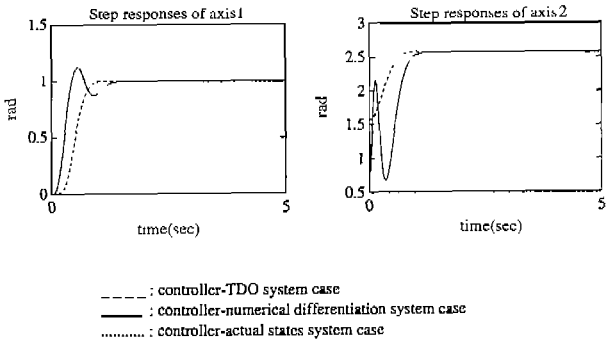

Fig. 2. Step response of two-dof manipulator with flexible joints using I/O linearization control without a modeling error.

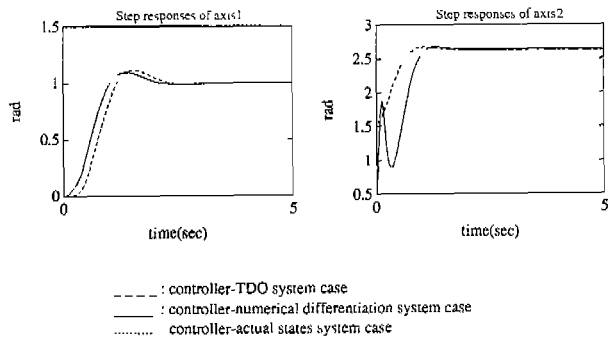

Fig. 3. Step response of two-dof manipulator with flexible joints using I/O linearization control with a 30% modeling error.

point of view. In contrast, the responses of the controller-numerical differentiation system are more oscillatory and show a larger overshoot. Fig. 3 shows that the modeling error results in sluggish responses (a larger overshoot), in all three of the control systems; yet, the responses of the controller-TDO system coincide with those of the benchmark, thereby demonstrating the robustness of the TDO to the modeling error. In comparison, the responses of the controller-numerical differentiation system show larger deviations from those of the benchmark.

In the second simulation, we applied the IOLTDC in two different cases: without a modeling error and with a 30% modeling error. Fig. 4 and 5 show the responses in these two cases. Similar to the responses of the IOLC, the responses of the controller-TDO system and the benchmark follow the desired responses well under the system without the modeling error, whereas those of the controller-numerical differentiation system are more oscillatory and show a larger overshoot (Fig. 4). This result confirms the advantage of using the TDO in designing the IOLTDC. Fig. 5 shows that the modeling error has little effect on the responses of the controller-TDO system and the benchmark, confirming that the robustness of the IOLTDC to the modeling error is maintained in the controller-TDO system and

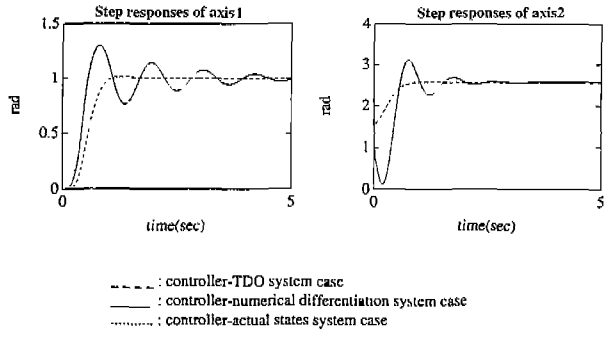

Fig. 4. Step response of two-dof manipulator with flexible joints using I/O linearization using TDC control without a modeling error.

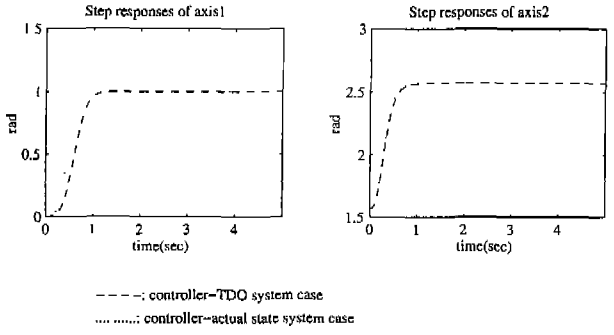

Fig. 5. Step response of two-dof manipulator with flexible joints using I/O linearization using TDC control with a 30% modeling error.

the benchmark. In contrast, the responses of the controller-numerical differentiation system are quite different from those without the modeling error and they also tend to diverge widely, so we did not plot their responses.

IV. Experiment

To test the performance of the TDO in a real system, we applied it to a two-dof SCARA robot system. This system is categorized into a MIMO plant in phase variable form. Thus, for the controller and observer design, the coordinate transformation is not required. In this experiment, the TDO was used in a position control loop *in conjunction with* the TDC, which requires velocity and acceleration to be reconstructed from the position measurement. The purpose of this experiment is twofold: to show that the TDO can be readily applied to the practical control areas and to investigate how it compares with another method that *does not require a model*, numerical differentiation which is also frequently used in practice.

The experimental system consists of the following components: Each joint of the robot, driven through harmonic drives with reduction ratios of 100:1 for joint 1 and 80:1 for joint 2, has a resolver with a resolution

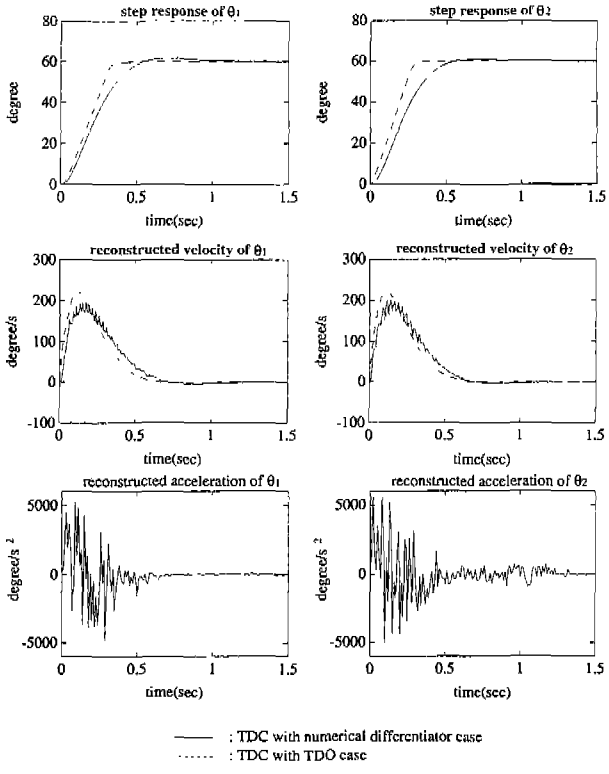

Fig. 6. Experimental results of a two-dof SCARA robot when step input is applied: the position responses, velocities and accelerations reconstructed with numerical differentiator and TDO.

of 4096 pulses/rev for position measurement. For links 1 and 2, the lengths are and l_1 = 35cm and l_2 = 20cm, the masses are m_1 = 11.17kg and m_2 = 6.82kg, the moments of inertia are I_1 = 1.03kgm^2 and I_2 = 0.224kgm^2, and the distances from the joints to the centers of the mass are L_1 = 30cm and L_2 = 28cm, respectively. For this robot, an accurate dynamic model is available [19]. The digital implementation of the TDO and TDC was made with the sampling frequency of 1000Hz in a multi-processor based system called CONDOR, which is described in detail in [22].

Fig. 6 shows the position responses, velocities, and accelerations of joint 1 and joint 2 with the numerical differentiation and TDO due to the step input of θ_{d1} = θ_{d2} = 60deg. As shown in Fig. 5, the control performance with the TDO is slightly better than that of the numerical differentiation in terms of overshoot and rising time. The reconstructed velocities and accelerations confirm that the TDO reconstructs the states smoothly and stably. By comparison, the numerical differentiation amplifies the sensor noise to a substantial degree.

V. Conclusion

This paper has developed an observer design method for nonlinear MIMO plants by applying trans-

formation into a GOBCF coupled with the TDO. The TDO method is extended from SISO plants in phase variable form [12] to MIMO plants in the general form of (1). As to the resulting TDO, the convergence of the observation error is analyzed and it is discussed that the resulting TDO has preserved the three merits (i.e., simplicity, numerical efficiency, and robustness) of the TDO, firstly introduced for SISO system.

The proposed TDO reconstructs states for the plant in the GOBCF without the real time computation of system nonlinearity. When the TDO is used for several control schemes based on the transformed coordinate, it can be designed even if the transformation is not known, and it only needs the transformability condition. Under these control structures, the proposed TDO can be easily implemented with faster sampling rate than other nonlinear observers.

Simulation results verify that the TDO is an effective observer for nonlinear MIMO systems. When the TDO is used together with an IOLC and IOLTDC, its control performance appears to be similar to those using actual states and superior to those using numerical differentiation. The TDO is, therefore, a promising observer design technique for the IOLC and IOLTDC. From the experiment on a robot position control, we have shown that the TDO may be effectively used in a real closed-loop system.

The limitations of the TDO occur when the states in the initial coordinate are reconstructed. In this case, the TDO needs a nonlinear coordinate transformation so that the inaccuracies in the plant model can reduce the state reconstruction performance. To take this limitation into account, research on the modification of the TDO is currently in progress.

References

[1] D. Bestle and M. Zeitz. Canonical form observer design for non-linear time-variable systems. *Int. J. Control*, 38(2):419-431, 1983.

[2] A. J. Krener and W. Respondek. Nonlinear observers with linearizable error dynamics. *SIAM J. Control and Optimization*, 23(2):197-216, 1985.

[3] H. Keller. Nonlinear observer design by transformation into a generalized observer canonical form. *Int. J. Control*, 46(6):1915-1930, 1987.

[4] M. Zeitz. Observability canonical (phase-variable) form for nonlinear time-variable systems. *Int. J. Systems Sci.*, 15(9):949-958, 1984.

[5] S. Nicosia, P. Tomei, and A. Tornambe. Feedback control of elastic robots by pseudo-linearization techniques. In *Proc. IEEE Conf. Decision Control*, pp. 397-340, 1986.

[6] C. Reboulet and C. Champetier. A new method for linearizing nonlinear systems: The pseudo-linearization. *Int. J. Control*, 40:631-638, 1984.

[7] W. T. Baumann and W. J. Rugh. Feedback Control of Nonlinear Systems by Extended Linearization. *IEEE Trans. Automatic Control*. AC31(1):343-361, 1984.

[8] J. -J. E. Slotine, J. K. Hedrick, and E. A. Misawa. On sliding observers for nonlinear systems. *ASME J. Dynamic Systems, Measurement and Control*, 109(3):245-252, 1987.

[9] C. Canudas de Wit and J. -J. E. Slotine. Sliding observers for robot manipulators. *Automatica*, 27 (5):859-864, 1991.

[10] B. L. Walcott and S. H. Zak. Combined observer-controller synthesis for uncertain dynamical systems with application. *IEEE Trans. Systems, Man, and Cybernetics*, 18(1):88-104, 1988.

[11] C. Canudas de Wit, N. Fixot, and K. J. Astrom. Trajectory tracking in robot manipulators via nonlinear estimated state feedback. *IEEE Trans. Robotics and Automation*, 8(1):138-144, 1992.

[12] P. H. Chang and J. W. Lee. Time delay observer: A robust observer for nonlinear plants. accepted to be published by *ASME J. Dynamic Systems, Measurement and Control*, 1997.

[13] K. Youcef-Toumi and O. Ito. A time delay controller design for systems with unknown dynamics. *ASME J. Dynamic Systems Measurement and Control*, 112(1):133-142, 1990.

[14] T. C. Hsia and L. S. Gao. Robot manipulator control using decentralized time-invariant time-delayed controller. In *Proc. of IEEE Int. Conf. Robotics and Automation*, pp. 2070-2075, 1990.

[15] J. Birk and M. Zeitz. Extended Luenberger observer for non-linear multivariable systems. *Int. J. Control*, 47(6):1823-1836, 1988.

[16] K. Youcef-Toumi and S. T. Wu. Input/output linearization using time delay control. *ASME J. Dynamic Systems Measurement and Control*, 114:10-19, 1992.

[17] J. -J. E. Slotine and Li. *Applied Nonlinear Control*. Prentice Hall, 1991.

[18] J. Y. Hung, W. Gao, and J. C. Hung. Variable structure control: A survey. *IEEE Trans. Industrial Electronics*, 40(1):2-22, 1993.

[19] S. Nicosia and P. Tomei. A nonlinear observer for elastic robot. *IEEE Trans. Robotics and Automation*, 4(1):45-52, 1988.

[20] K. Youcef-Toumi and S. Reddy. Stability analysis of TDC with application to high speed bearing. In *ASME Winter Annual meeting*, 1990.

[21] P. H. Chang and J. W. Lee. A model reference observer for time-delay control and its application to robot trajectory control. *IEEE Trans. Control System Technology*, 4(1):2-10, 1996.

[22] S. Narasimhan, D. M. Siegel, and J. M. Hollerbach. Condor: An architecture for controlling the Utah-MIT dexterous hand. *IEEE Trans. Robotics and Automation*, 5(5):616-627, 1989.

Appendix

Proof of Lemma 1: Subtracting equation (5) from equation (14), the observation error dynamics for i-th subsystem becomes

$$\dot{\mathbf{e}}_i = (\mathbf{E}_{n_i} + \mathbf{K}_i\mathbf{C}_i)\mathbf{e}_i + \alpha_i\mathbf{R}_i\dot{\mathbf{e}}_{i(t-L)} - \Phi_i(\mathbf{z},\bar{\mathbf{u}}), \tag{29}$$

where $\mathbf{R}_i$ denotes an $n_i \times n_i$ matrix, all the elements of which are zero except for $\mathbf{R}_i(n_i \times n_i) = 1$ and

$$\Phi_i(\mathbf{z},\bar{\mathbf{u}}) = \left[\mathbf{0}_{1\times(n_i-1)} \vdots (1-\alpha_i)a_i(\mathbf{z},\bar{\mathbf{u}}) - \alpha_i\phi_i(\mathbf{z},\bar{\mathbf{u}},L)\right]^T. \tag{30}$$

Since $\dot{\mathbf{e}}_{i(t-L)} = \dot{\mathbf{e}}_i - [\dot{\mathbf{e}}_i - \dot{\mathbf{e}}_{i(t-L)}]$, (29) may be expressed as

$$\begin{aligned}(\mathbf{I}_{n_i} - \alpha_i\mathbf{R}_i)\dot{\mathbf{e}}_i &= (\mathbf{E}_{n_i} + \mathbf{K}_i\mathbf{C}_i)\mathbf{e}_i \\ &\quad - \alpha_i\mathbf{R}_i\left[\dot{\mathbf{e}}_i - \dot{\mathbf{e}}_{i(t-L)}\right] - \Phi_i(\mathbf{z},\bar{\mathbf{u}}).\end{aligned} \tag{31}$$

For a sufficiently small L that guarantees the continuity assumption of $a_i(\mathbf{z},\bar{\mathbf{u}})$, it holds that $\frac{\dot{\mathbf{e}}_i - \dot{\mathbf{e}}_{i(t-L)}}{L} = \ddot{\mathbf{e}}_i - O(L^2)$, which is used to rearrange (31) into the following:

$$\begin{aligned}\alpha_i L\mathbf{R}_i\ddot{\mathbf{e}}_i + (\mathbf{I}_{n_i} - \alpha_i\mathbf{R}_i)\dot{\mathbf{e}}_i &= (\mathbf{E}_{n_i} + \mathbf{K}_i\mathbf{C}_i)\mathbf{e}_i \\ &\quad + \alpha_i L\mathbf{R}_i O(L^2) - \Phi_i(\mathbf{z},\bar{\mathbf{u}}),\end{aligned} \tag{32}$$

Define a new state variable $e_{in_i+1} = \dot{e}_{n_i}$, then the last equation in (32) becomes

$$\begin{aligned}\dot{e}_{in_i} &= e_{in_i+1} \\ \dot{e}_{in_i+1} &= \frac{K_{in_i}}{\alpha_i L}e_{i1} - \frac{(1-\alpha_i)}{\alpha_i L}e_{in_i+1} - \frac{(1-\alpha_i)}{\alpha_i L}a_i(\mathbf{z},\bar{\mathbf{u}}) \\ &\quad - \psi_i(L) + \frac{\alpha_i}{\alpha_i L}\phi_i(\mathbf{z},\bar{\mathbf{u}},L)\end{aligned} \tag{33}$$

Combining (33) with (32) leads to the aforementioned error dynamics (16). (Q.E.D.)

Proof of Theorem 1: Since the distinct eigenvalues of $\tilde{\mathbf{A}}_i$ have negative real parts, there exists a transform matrix $\mathbf{T}_i$ that diagonalizes $\tilde{\mathbf{A}}_i$, namely

$$\Lambda_i = \mathbf{T}_i\tilde{\mathbf{A}}_i\mathbf{T}_i^{-1}, \tag{34}$$

where Λ_i is a diagonal matrix whose diagonal elements are the eigenvalues of $\tilde{\mathbf{A}}_i$. By using $\mathbf{T}_i$, (16) can be transformed to

$$\dot{\boldsymbol{\varepsilon}}_i = \Lambda_i\boldsymbol{\varepsilon}_i - \mathbf{T}_i\tilde{\mathbf{B}}_i\gamma_i(\mathbf{z},\bar{\mathbf{u}},L), \tag{35}$$

where

$$\boldsymbol{\varepsilon}_i = \mathbf{T}_i\tilde{\mathbf{e}}_i. \tag{36}$$

Defining a Lyapunov function as $V_i = -\frac{1}{2}\boldsymbol{\varepsilon}_i^T\Lambda_i^{-1}\boldsymbol{\varepsilon}_i$ and using (34), (35), and (36), may be obtained as follows:

$$\begin{aligned}\dot{V}_i &= -\frac{1}{2}\boldsymbol{\varepsilon}_i^T\left(\Lambda_i^T\Lambda_i^{-1} + \Lambda_i^{-1}\Lambda_i\right)\boldsymbol{\varepsilon}_i + \boldsymbol{\varepsilon}_i^T\Lambda_i^{-1}\mathbf{T}_i\tilde{\mathbf{B}}_i\gamma_i(\mathbf{z},\bar{\mathbf{u}},L) \\ &= -\boldsymbol{\varepsilon}_i^T\boldsymbol{\varepsilon}_i + \boldsymbol{\varepsilon}_i^T\mathbf{T}_i^{-1}\tilde{\mathbf{A}}^{-1}\tilde{\mathbf{B}}_i\gamma_i(\mathbf{z},\bar{\mathbf{u}},L).\end{aligned} \tag{37}$$

The inverse of $\tilde{\mathbf{A}}_i$ can be symbolically obtained as follows:

$$\tilde{\mathbf{A}}_i^{-1} = \begin{bmatrix}\mathbf{0}_{1\times(n_i-1)} & \vdots & -\frac{1-\alpha_i}{K_{in_i}}\mathbf{v}_i & \vdots & -\frac{\alpha_i L}{K_{in_i}}\mathbf{v}_i \\ \mathbf{I}_{n_i} & \vdots & 1 & \vdots & 0 \\ \mathbf{0}_{1\times(n_i-1)} & \vdots & 1 & \vdots & 0\end{bmatrix}, \mathbf{v}_i = \begin{bmatrix}-1 \\ K_{i1} \\ \vdots \\ K_{in_i}\end{bmatrix}.$$

Using the matrix norm properties together with (17) and (36), (37) leads to

$$\begin{aligned}\dot{V}_i &\le -\|\boldsymbol{\varepsilon}_i\|^2 + \|\boldsymbol{\varepsilon}_i\|\|\mathbf{T}_i\|\left\|\tilde{\mathbf{A}}_i^{-1}\tilde{\mathbf{B}}_i\gamma_i(\mathbf{z},\bar{\mathbf{u}},L)\right\| \\ &< -\|\mathbf{T}_i\tilde{\mathbf{e}}_i\|\left\{\|\mathbf{T}_i\tilde{\mathbf{e}}_i\| - \|\mathbf{T}_i\|\sqrt{\frac{(1+K_{i1}^2+\cdots+K_{in_i-1}^2)}{K_{in_i}^2}}\beta_i\right\}.\end{aligned} \tag{38}$$

Hence, for any that satisfies

$$\|\tilde{\mathbf{e}}_i\| \ge \|\mathbf{T}_i\|^{-1}\|\mathbf{T}_i\|\sqrt{\frac{(1+K_{i1}^2+\cdots+K_{in_i-1}^2)}{K_{in_i}^2}}\beta_i = \delta_i.$$

$\dot{V}_i$ remains negative, causing $\tilde{\mathbf{e}}_i$ to converge to $\mathbf{B}_i(\delta_i)$.

In addition, the steady state error can be derived from (15) as follows:

$$\tilde{\mathbf{e}}_{i_{ss}} = \tilde{\mathbf{A}}_i^{-1}\tilde{\mathbf{B}}_i\gamma_i(\mathbf{z},\bar{\mathbf{u}},L)_{ss}. \tag{39}$$

Using (39) and (17) together with the upper bounds of $|a_i(\mathbf{z},\bar{\mathbf{u}})|$, $|\psi_i(L)|$, $|\phi_i(\mathbf{z},\bar{\mathbf{u}})|$, one can immediately obtain the steady state observation error in (20). (Q.E.D.)

Jeong Wan Lee

He received B.S. degree in mechanical design and production engineering from Seoul National University, in 1989, the M.S. degree in precision engineering and mechatronics from KAIST, in 1992, and the PhD degree in mechanical engineering from KAIST, Korea, in 1998. Since 1999, he has been a full-time lecturer with the division of mechanical engineering and mechatronics, Kangwon National University. His research interests include robotics, observer based control, and robust control application.

Pyung Hun Chang

He received the B.S. and M.S. degrees in mechanical engineering from Seoul. National University, in 1974 and 1977, respectively. He received Ph.D. degree in mechanical engineering from Massachusetts Institute of Technology, Cambridge, MA, in 1987. From 1984 to 1987, he was involved in a research project in the field of robotics as a research assistant at the Artificial Intelligence Laboratory (AI Lab) of MIT. Since 1987, he has been an associate professor with the department of mechanical engineering, Korea Advanced Institute of Science and Technology (KAIST), Taejon, Korea. His research interests include the control of redundant robots, high accuracy/speed control with application to mechanical systems, robust control of nonlinear plants, and observer based controls.